

Published in final edited form as:

Trends Biotechnol. 2012 March ; 30(3): 138–146. doi:10.1016/j.tibtech.2011.06.013.

Self-folding devices and materials for biomedical applications

Christina L. Randall¹, Evin Gultepe², and David H. Gracias^{2,3}

¹Department of Biomedical Engineering, The Johns Hopkins University, Baltimore, MD 21205

²Department of Chemical and Biomolecular Engineering, Johns Hopkins University, Baltimore, MD 21218, USA

³Department of Chemistry, Johns Hopkins University, Baltimore, MD 21218, USA

SUMMARY

Since the native cellular environment is three dimensional (3D), there is a need to extend planar, micro and nanostructured biomedical devices to the third dimension. Self-folding methods can extend the precision of planar lithographic patterning into the third dimension and create reconfigurable structures that fold or un-fold in response to specific environmental cues. Here, we review the use of hinge-based self-folding methods in the creation of functional 3D biomedical devices including precisely patterned nano to centimeter scale polyhedral containers, scaffolds for cell culture, and reconfigurable surgical tools such as grippers that respond autonomously to specific chemicals.

Precisely structured biomedical devices and materials

One of the challenges in advancing biomedical engineering is the construction of miniaturized, patterned and biologically relevant three dimensional (3D) devices and materials. Conventional microfabrication methods enable devices to be patterned down to the nanoscale, but in an inherently two dimensional (2D) manner [1]. As a result, while precisely engineered microwell arrays [2] and bio-artificial organs [3] are defined as 3D recesses, they feature lithographically defined porosity only along one surface, which can result in hypoxic conditions for cells residing far away from this surface [4]. For drug delivery, microfabricated controlled-release implantable devices have been developed [5], but drug diffusion to the surroundings is also constrained through only one planar opening. Hence, to increase molecular perfusion with the surroundings, while retaining small sizes, there is a need to precisely define side-wall porosity of microfabricated microwells, bio-artificial organs and drug delivery reservoirs in three dimensions.

Existing 3D polymeric and gel-based particulates used in drug delivery offer limited precision in their size, shape and porosity. Nanoparticles can be synthesized in the shape of spheres, tripods and rods [6, 7], but it is still challenging to create monodisperse micro and nanoparticles with controlled patterns of materials with heterogeneous composition. Three dimensional lithographic structuring offers the possibility for unprecedented precision in the size, shape, surface patterns, and porosity of particles for controlled release and targeted therapeutics.

© 2011 Elsevier Ltd. All rights reserved.

Corresponding author: Gracias, D. H. (dgracias@jhu.edu).

Publisher's Disclaimer: This is a PDF file of an unedited manuscript that has been accepted for publication. As a service to our customers we are providing this early version of the manuscript. The manuscript will undergo copyediting, typesetting, and review of the resulting proof before it is published in its final citable form. Please note that during the production process errors may be discovered which could affect the content, and all legal disclaimers that apply to the journal pertain.

The human body is a 3D structure and elaborately patterned from the nano to the macroscale. Tissues are not homogeneous, flat petri-dishes; hence, the generation of materials that are precisely structured, at a hierarchy of length scales in 3D, are essential to the development of accurate models to replicate in-vivo cell behavior [8]. There is also a need to create 3D models of tissue in anatomically relevant geometries, such as the complex folds observed in skin or microvilli. Concurrently, there is a need to integrate vasculature and chemical patterning into these 3D structures to simulate in-vivo growth and proliferation conditions. Self-assembly techniques can complement existing 3D tissue fabrication and patterning methods [9–12] by providing a highly parallel mechanism to assemble complex 3D scaffolds with micro and nanoscale features.

In surgery, there is a push for further miniaturization of tools to allow for less invasive procedures and enable access to hard-to-reach areas within the human body. Additionally, if tetherless, stimuli-responsive, miniaturized tools can be created, it may be possible to realize the futuristic vision of an “autonomous miniaturized surgeon” or truly non-invasive surgery [13–14].

Self-folding refers to self-assembly processes wherein planar structures fold up spontaneously, typically when released from a substrate or exposed to specific stimuli. The driving forces for self-folding can be varied and result from material heterogeneities that are either stimulated or engineered during fabrication [15]. Self-folding of hingeless structures results in curved or rolled-up structures whereas the introduction of micro and nanoscale hinges results in structures with discrete folds. As in other self-assembly methods, the challenge is to realize a small set of outcomes, typically just one desired 3D material or device, from many possibilities. This review focuses on the concept of combining the precision of planar lithographic methods with hinge-based self-folding to develop precisely engineered and three dimensionally patterned biomedically relevant structures in a highly parallel and cost-effective manner. We restrict our discussion to self-folding methods that do not employ electrical or pneumatic control so that the structures formed need not be substrate bound or tethered. The creation of permanently bonded and reconfigurable self-folded structures in the form of hollow polyhedral containers, scaffolds, and tetherless surgical tools is described; self-folding is driven by heating or on exposure to specific chemical stimuli.

Self-folding polyhedral containers

The motivation for developing self-folding polyhedral micro/nanoscale containers is to utilize the extreme precision of planar lithographic methods to precisely structure hollow encapsulants in all three dimensions. There are multitudes of metallic, inorganic, polymeric and gel-based spherical structures, such as nanoparticles, liposomes and microspheres that have been utilized for the encapsulation or binding of therapeutic cargo [16, 17]. While many of these systems have excellent characteristics, including biocompatibility and biodegradability, there are challenges with engineering reproducible formulations that enable a range of sizes, shapes and pharmaco-kinetic properties [18, 19]. For example, gel-based encapsulants feature porosity that is a consequence of physical or chemical cross-linking which is subject to batch-to-batch variability and poly-dispersivity in pore or particle size [17]. Similarly, it can be challenging to obtain homogenous and reproducible particle sizes in liposomal assembly [18]. Recent studies have also argued that the shape and size of therapeutic particles is important in determining their efficacy and bio-distribution [20, 21]. Hence, an emerging research thrust is focused on the development of methods to precisely control the shape of micro and nanoparticles for drug delivery [22–23], and the push towards lithographic patterning of encapsulants is emerging [24]. While these new methods allow for polymeric and gel-based particles to be manufactured with precision, they still do not enable

precise patterning of pores in all three dimensions. Moreover, these methods result in solid cross-linked structures rather than hollow encapsulants. As a result chemicals are encapsulated within the cross-linked gel or polymer matrix, and chemical loading is strongly dependent on the molecular/chemical properties of the pharmaceutical and the matrix, as well as the matrix synthesis process.

Lithography in combination with self-folding allows for the engineering of hollow encapsulants with precise and reproducible shape, size, surface patterns and porosity. Precisely patterned, hollow polyhedra with overall sizes ranging from 100 nm to 1 cm can be fabricated with a variety of materials, including metals, ceramics and polymers [15, 25–26]. Highly parallel self-folding allows large numbers of polyhedra to be fabricated simultaneously on a single substrate. Arbitrary patterns can be designed with heterogeneous materials to serve as sensory or communicable modules or etched away to serve as pores. The pattern resolution is limited only by the lithographic process and patterns as small as 15 nm have been defined on the faces of hollow cubic particles using electron beam lithography [25]. In order to self-fold polyhedra from planar templates, the predominantly utilized forces are generated by either the minimization of surface energy [27] or by the release of thin film stress [28]. The versatility of the approach is depicted in Figure 1 and the two methods are discussed in subsequent sections.

Surface tension based self-folding methodology (Fig. 1a) derives inspiration from earlier research in MEMS [29] and the folding of solid polyhedra around droplets of solder [30]. However, the introduction of self-aligning, locking hinges [27, 31] has led to the development of well-sealed, mechanically robust, hollow polyhedra that can be manipulated without breaking. The creation of polyhedra with well sealed and non-leaky seams is critical to realize chemical release only through lithographically patterned pores. Briefly, a low melting point material is deposited in-between panels (folding hinges, Fig. 1b1), and at their edges (locking hinges, Fig. 1b2) to create a 2D template or net. Compact nets for a specific polyhedron have been observed to self-fold with high yields [32]. After planar fabrication, the nets are released from the substrate and heated to liquefy the solid hinges. The use of low melting polymeric hinges such as those composed of biodegradable polycaprolactone (PCL) along with SU-8 photoresist (an epoxy based polymer) panels have extended this methodology to the design of all-polymeric containers with precisely defined wall porosity [26] (Figure 1c–d). These polymeric containers resemble miniaturized 3D petri-dishes, are bioinert and optically transparent for easy visualization of encapsulated cells (Figure 1e). For in-vivo applications, the use of biodegradable hinges facilitates the disintegration of containers over time, offering the possibility of tailoring the clearance from the body.

The polyhedra are mechanically strong because the liquefied locking hinges at the edges of panels fuse and subsequently harden. Additionally, locking hinges enhance self-correction and cooperativity during folding and allow for the development of more complex polyhedra [33] (Figure 1f–g). A plasma-etching driven heating process, in vacuum, has realized self-folding of 100 nm scale hollow containers with precisely patterned surfaces [25] (Figure 1h–i). Here, well defined, molecular functionalized patterns on polyhedral nanoscale encapsulants can, in principle, be used to define specific recognition or evasion sites for targeted therapeutics.

Self-folding containers can also be formed by utilizing hinges composed of differentially stressed bilayers [28]; self-folding occurs due to release of residual stress [34]. The incorporation of a polymeric trigger on the stressed hinges enables stimuli-responsive self-folding, allowing for simultaneous loading while folding. Heat induced softening of the polymer during self-folding causes the edges of panels to fuse, resulting in more mechanically robust containers. Stressed hinges have been utilized to form containers that

self-loaded live fibroblast cells and *Triops* embryos [35]. Self-loading can be thought of as the statistical process of encapsulation during self-assembly, and it is an advantage of stress-driven assembly. In the event that the folding conditions require higher temperatures, hollow polyhedral containers can be loaded after self-folding using micromanipulators [36], by tumbling or autonomous motion [37, 38] or by allowing the cargo to settle into them, followed by a subsequent sealing step.

We highlight applications that exploit the advantageous features offered by the self-folding process such as versatility in size, shape, material composition and precise 3D patterning. Due to the large size range of polyhedra that can be formed by this self-folding method, hollow containers can be used to encapsulate a range of biological cargos. Since, containers can be fabricated with ferromagnetic materials such as nickel, they can be remotely manipulated and heated using electromagnetic fields. As a result, chemicals have been locally delivered to live cells at the push of a button without detriment [39–40]. Additionally, both in-vitro and in-vivo magnetic resonance imaging (MRI) were performed and device tracking was possible during flow in a microfluidic channel [27, 41]. Furthermore, devices as small as 50 μm were imaged with computed axial tomography [40].

Applications that leverage precise pore patterning on the faces of the containers in all three dimensions have been explored. Due to the utilization of standard lithographic techniques, containers with precisely defined porosity on each face of cubic containers have been designed to elucidate the effects of oxygen diffusion on encapsulated cells [38]. Cell viability and insulin release from cells encapsulated within cubic containers with one, three and five porous faces were compared. The one porous-faced containers mimic existing planar reservoirs or microwells while the five porous-faced containers represent 3D microwells (Figure 2a). Arrays of these self-folded containers could be formed on both rigid/flat (Figure 2b) and flexible/curved substrates (Figure 2c). β -TC-6 insulinoma cells were encapsulated within these Au-coated, polyhedral arrays and a significantly higher insulin release was observed from five porous-faced microwells as compared to three and one porous-faced microwells (Figure 2d–e). It should be noted that insulinoma cells prefer to aggregate in clusters rather than spread on surfaces; hence, in liquid media within the containers, these cells grew into 3D clusters, in the absence of a synthetic biomaterial matrix. Higher insulin release was correlated to a higher fraction of viable cells encapsulated in 3D microwells as compared to their 2D counterparts due to enhanced oxygen diffusion from five faces as compared to one face. This demonstration clearly highlights the need to develop cell encapsulation devices that permit diffusion in three dimensions for enhanced cell viability.

Precisely patterned polyhedral containers have also been used to generate 3D chemical patterns for cellular self-organization [42]. The in-vitro generation of 3D chemical patterns within liquid or gel media is important to understanding chemotaxis, cell signaling, angiogenesis, homeostasis, and immune surveillance [43–47]. Since self-folding methods enable porosity to be precisely realized in three dimensions, chemicals emerge from the containers, by diffusion, with unprecedented spatio-temporal characteristics that are controlled by the size of the container, pore-size, pore-density and pore-placement [42]. Diffusion based spatio-temporal controlled release of chemicals in precise 3D patterns such as conical gradients and helices has been realized. Additionally, a helical pattern of L-serine served as a chemical scaffold to direct self-organization of E-coli bacteria into a helical pattern (Figure 3a–d).

Containers can be loaded by immersing them into the desired chemical, washed and re-used. As compared to loading of chemicals in cross-linked gels or polymers, due to the physical entrapment of the chemical in these hollow containers, different classes of chemicals can be

encapsulated. As a result, containers have been used to release fluorescent dyes, chemoattractants, bacterial broths, cellular media, therapeutic proteins and antibodies. In one case, insulin and IgG were both loaded into containers by simply soaking them in a solution containing the two chemicals; release of both IgG and insulin was subsequently verified. While it is possible to load and release more than one chemical from existing cross-linked polymer matrix constituted drug delivery systems, the process can be more complicated and time-consuming [48].

Anatomically relevant 3D patterned scaffolds

It is becoming increasingly clear that three dimensionality and the mechanical properties of tissue scaffolds are important in regulating cellular behavior [45, 49–51]. For example, it has been reported that 3D tumor models created by culturing carcinoma cells within porous poly(lactide-co-glycolide) more accurately resembled tumors formed in-vivo. Additionally, such 3D tumors models were less sensitive to chemotherapeutic drugs as compared to planar models [46]; this result has important implications for in-vitro tissue models used in drug screening. Hence, a major thrust is to move in-vitro cell culture away from flat petri-dishes to the third dimension. As a result, a large number of methods, such as the aforementioned porous hydrogel blocks, electrospinning [52], cell sheet engineering [53] and direct-write methods [54] are being developed for tissue engineering applications. Nevertheless, it is still challenging to create the intricate and anatomically relevant scaffolds that incorporate the complex architecture and mechanical property heterogeneity observed in real tissues.

Self-folding methods have been utilized to create precisely patterned scaffolds in anatomically relevant geometries, namely cylinders (vasculature, ducts), spirals (glandular coils, cochlea), and bidirectionally folded sheets (gyri/sulci, villi) [55–56]. A schematic of the approach is shown in Figure 4a. Multiple layers of lithography are utilized to structure materials with differential stress, incorporated into hundreds to even thousands of hinges, so that the entire scaffold self-assembles into the desired architecture when released from the substrate. Published mechanics models [57] allow an estimation of the radius of curvature within each hinge to achieve arbitrary positive or negative local or global curvature and self-fold sheets with bi-directional curvature [58]. Scaffolds from bioinert materials have been self-folded and subsequently coated them with extra cellular matrix proteins such as fibronectin to enable cell culture in anatomically relevant 3D geometries (Figure. 4b–g). The morphology of fibroblast cells cultured on these scaffolds was imaged using both fluorescence and electron microscopy. Significant morphological differences were observed on scaffolds patterned with different materials, as measured by cell spreading and the number of filipodia expressed on the cell surface. Additionally, it was observed that fibroblast cells could form connections to adjacent cells on the same fold surface, as well as bridge the gap between nearby folds, pointing towards the capability of cells to form more cell-cell connections when cultured in 3D folded geometries [56].

Reconfigurable self-folding devices as surgical tools

In addition to the permanently bonded structures described above, self-folding methods can also be utilized to create reconfigurable 3D structures; efforts have been focused on the development of small tools to enable less-invasive surgical procedures. Minimally invasive surgery (MIS) has achieved pre-eminence because it reduces the length of hospitalization, lowers the associated costs, decreases post-surgery pain and improves the cosmetic result [59–62]. Surgery is an evolving field and continues toward even less invasive methods [63–65]. Since the dimensions of surgical tools often dictate the incision size, the progress in the evolution of MIS to achieve efficient and effective access to the surgical area is closely linked to the developments in micro/nanoengineering [66]. MIS also often requires many

instruments including light sources, cameras and surgical tools operated simultaneously through a small hole [67]. The challenges created by this crowded surgical environment can be overcome by designing innovative imaging systems and miniaturized surgical devices [14, 68].

Tetherless and thermally or chemically actuated self-folding tools have been fabricated by interconnecting rigid panels with flexible joints composed of stressed multilayered, metallic thin-films [69–72]. The shapes of the self-folding tools were modeled after biological appendages, such as hands, in which the jointed digits were arranged around a central palm; hence they were named microgrippers. The folding of the microgrippers could be triggered by heating or on exposure to a variety of chemicals. All triggering mechanisms altered the mechanical properties of a polymeric trigger layer and allowed control over the release of the stress in the metallic films. Thus, multilayer-jointed microgrippers remained open until they were triggered. It was also possible to both fold or close and un-fold or open these microgrippers by designing bi-directional hinges [70]. Alternate mechanisms such as surface modification of thin film hinges can enable closing and opening of chemically responsive microgrippers reversibly over multiple cycles [72]; however, this feature has yet to be demonstrated under surgically relevant conditions.

In addition to autonomous actuation on exposure to appropriate chemicals, magnetic guidance has allowed microgrippers with embedded ferromagnetic layers to be navigated in small, twisted passages without the need for a tether. Figure 5(a–e) shows a microgripper that was remotely guided into a capillary tube and thermally triggered to excise a portion of living cell mass. The microgripper was subsequently guided out of the capillary with the captured cells in its grasp; Figure 5f shows the fluorescent micrograph of the retrieved gripper closed around live Calcein stained (green) L929 cells after 4h in media.

The utility of the self-folding microgrippers as surgical tools was further explored by in-vitro and ex-vivo procedures intended to simulate biopsies. An in-vitro biopsy was performed by utilizing the microgrippers to excise cells from a bovine bladder tissue sample. A magnet was used to rotate the gripper such that the claws could cut into the tissue and subsequently remove a sample. Figure 5g shows the gripper with retrieved tissue after the successful biopsy procedure. For in-vivo biopsies, it is conceivable that microgrippers could be deployed and retrieved endoscopically by exploiting their magnetic guidance and autonomous actuation features. A preliminary result shows the grippers within the intrahepatic bile ducts after deployment through a catheter into the common bile duct, in an ex-vivo porcine model (Figure 5h–i).

Self-folding microgrippers can be tailored to respond to more specific biochemical cues with the ultimate goal of autonomous disease-responsive function. Biopolymeric trigger layers have been utilized in order to leverage the specificity of enzyme substrate reactions thereby increasing the actuation selectivity of self-folding microgrippers [70]. Here, grippers were fabricated with hinges composed of biopolymers that were degraded only by specific enzymes. These grippers contained two sets of pre-stressed metallic hinges capped with two different biopolymeric triggers that were targeted by different families of enzymes including proteases, such as collagenase. The biopolymers of the trigger layers were chosen such that the presence of the first enzyme actuated only the first set of hinges causing the gripper to fold or close and without affecting the second set. When the second enzyme was introduced to the medium, the biopolymer triggers within the second set of hinges were attacked, and these hinges also curved, but in the opposite direction, causing the gripper to un-fold or open. Figure 6(a–f) shows the optical images and schematic representation of the enzyme actuated self-folding grippers. The response of the grippers to different enzymes indicates high actuation specificity (Figure 6g).

These self-folding tetherless microgrippers are promising candidates for realizing the vision of combining biochemical sensing and mechanical actuation so that they can discriminate between biomarkers and autonomously respond at diseased sites to perform simple surgical tasks.

Conclusions and future outlook

In conclusion, hinge-based self-folding strategies enable the transformation of precisely patterned, planar lithographic structures from 2D to 3D, thus creating miniaturized 3D biomedical structures such as encapsulants, particles, scaffolds and surgical tools. Considerable versatility and numerous strengths of the approach have been demonstrated; however, future challenges abound. One challenge lies in the creation of 2D templates composed of polymers and hydrogels so that self-folding structures can be constructed using a wider range of biocompatible and biodegradable materials. This challenge arises from the fact that planar lithographic methods have been primarily developed for the microelectronics industry and, as a consequence are not as well developed for use with biological materials. One possible solution path is the molecular synthetic modification of polymers and gels and the addition of cross-linkers and polymerization initiators to facilitate optical patterning using photolithography [71, 73–74]. Alternatively these materials could be patterned by soft-lithographic methods such as molding or stamping [23, 75–77]. Some of these methods have been utilized to fabricate hingeless polymeric structures that roll-up or curve spontaneously [73, 74, 76]. Despite these promising, recently-developed methods, the lithographic planar patterning of biomaterials, especially at the nanoscale, is in its infancy. Another challenge is the generation and manipulation of stress to achieve different magnitudes of curvatures especially for self-folding of nanoscale devices. Moreover, self-folding materials and devices composed of hydrogels could swell or collapse when exposed to different solvents. In some applications, such as drug delivery, this feature may be useful, whereas in others such as cell encapsulation therapy, additional cross-linking steps would be required to improve mechanical rigidity and stability over long implant durations. The use of self-aligning locking hinges provides an attractive means to increase mechanical strength. In this review, we have focused our discussion on substrate-free self-folding schemes; however, self-folding of wired electrochemically actuated polymers [78] provide considerable promise for substrate-bound and arrayed devices.

In order to enable autonomous surgical tools, there are a plethora of challenges in designing strategies for autonomous motion, guidance, data transfer and retrieval. Hence, the integration of microgrippers with communicable modules [79], the exploration of strategies to autonomously move micro and nanostructures [80] and the incorporation of novel biopolymers to enable actuation in response to disease markers such as cytokines expressed at sites of inflammation need to be further explored. The creation of autonomous surgical tools will also require heterogeneous integration across length scales, so that diverse materials such as metals for sharp tips for excision, semiconductors for information processing and memory and biopolymers or hydrogels as triggers can be incorporated into the same miniaturized tool. Such heterogeneous integration represents a big challenge since these different material classes have very different mechanical properties, thermal stability and chemical solubilities. Nevertheless, we believe that these and other challenges will be overcome as the methods of micro and nanoscale engineering become more pervasive in bioengineering and medicine.

Acknowledgments

We acknowledge funding from the NIH Director's New Innovator Award Program, part of the NIH Roadmap for Medical Research, through grant number 1-DP2-OD004346-01. Information about the NIH Roadmap can be found at <http://nihroadmap.nih.gov>. We thank Mustapha Jamal for help with figure preparation.

REFERENCES

1. Madou, MJ. Fundamentals of microfabrication: the science of miniaturization. 2nd ed. CRC Press; 2002.
2. Charnley M, et al. Integration column: microwell arrays for mammalian cell culture. *Integr Biol*. 2009; 1:625–634.
3. Desai TA, et al. Microfabricated immunoisolating biocapsules. *Biotechnol Bioeng*. 1998; 57:118–120. [PubMed: 10099185]
4. Rappaport C. Review—Progress in concept and practice of growing anchorage-dependent mammalian cells in three dimensions. *In Vitro Cell Dev Biol Anim*. 2003; 39:187–192. [PubMed: 12880369]
5. Santini JT, et al. Microchips as controlled drug-delivery devices. *Angew Chem Int Ed Engl*. 2000; 39:2396–2407. [PubMed: 10941095]
6. Choi CL, Alivisatos AP. From artificial atoms to nanocrystal molecules: Preparation and properties of more complex nanostructures. *Annu Rev Phys Chem*. 2010; 61:369–389. [PubMed: 20055683]
7. Xia Y, et al. Shape-controlled synthesis of metal nanocrystals: Simple chemistry meets complex physics? *Angew Chem Int Ed Engl*. 2008; 48:60–103. [PubMed: 19053095]
8. Leong KF, et al. Solid freeform fabrication of three-dimensional scaffolds for engineering replacement tissues and organs. *Biomaterials*. 2003; 24:2363–2378. [PubMed: 12699674]
9. Nichol JQ, Khademhosseini A. Modular tissue engineering: engineering biological tissues from the bottom up. *Soft Matter*. 2009; 5:1312–1319. [PubMed: 20179781]
10. Chan V, et al. Three-dimensional photopatterning of hydrogels using stereolithography for longterm cell encapsulation. *Lab Chip*. 2010; 10:2062–2070. [PubMed: 20603661]
11. Tsang VL, Bhatia SN. Fabrication of three dimensional tissues. *Adv Biochem Eng Biotechnol*. 2007; 103:189–205. [PubMed: 17195464]
12. Annabi N, et al. Controlling the porosity and microarchitecture of hydrogels for tissue engineering. *Tissue Eng Part B Rev*. 2010; 16:371–383. [PubMed: 20121414]
13. Feynman RP. There's plenty of room at the bottom. *J Microelectromech Syst*. 1992; 1:60–66.
14. Fernandes R, Gracias DH. Toward a miniaturized mechanical surgeon. *Mater Today*. 2009; 12:14–20.
15. Leong TG, et al. Three-dimensional fabrication at small size scales. *Small*. 2010; 7:792–806. [PubMed: 20349446]
16. Malam Y. Liposomes and nanoparticles: nanosized vehicles for drug delivery in cancer. *Trends Pharmacol Sci*. 2009; 30:592–599. [PubMed: 19837467]
17. Coelho JF, et al. Drug delivery systems: Advanced technologies potentially applicable in personalized treatments. *EPMA J*. 1:164–209.
18. Sharma A, Sharma US. Liposomes in drug delivery: progress and limitations. *Int J Pharm*. 1997; 154:123–140.
19. Hoarea TR, Kohaneb DS. Hydrogels in drug delivery: Progress and challenges. *Polymer*. 2008; 49:1993–2007.
20. Gao H, et al. Mechanics of receptor-mediated endocytosis. *Proc Natl Acad Sci USA*. 2005; 102:9469–9474. [PubMed: 15972807]
21. Champion JA, Mitragotri S. Role of target geometry in phagocytosis. *Proc Natl Acad Sci USA*. 2006; 103:4930–4934. [PubMed: 16549762]
22. Sanhai W, et al. Seven Challenges for Nanomedicine. *Nat Nanotechnol*. 2008; 3:242–244. [PubMed: 18654511]

23. Champion JA, et al. Making polymeric micro- and nanoparticles of complex shapes. *Proc Natl Acad Sci USA*. 2007; 104:1901–1904. [PubMed: 17264213]
24. Jeong W, et al. Challenging Nature's Monopoly on the Creation of Well-defined Particles. *Nanomedicine*. 2010; 5:633–639. [PubMed: 20528457]
25. Cho JH, Gracias DH. Self-assembly of lithographically patterned nanoparticles. *Nano Lett*. 2009; 9:4049–4052. [PubMed: 19681638]
26. Azam A, et al. Self-folding micropatterned polymeric containers. *Biomed Microdevices*. 2010; 13:51–58. [PubMed: 20838901]
27. Gimi B, et al. Self-assembled three-dimensional radio frequency (RF) shielded containers for cell encapsulation. *Biomed Microdevices*. 2005; 7:341–345. [PubMed: 16404512]
28. Leong TG, et al. Thin film stress driven self-folding of microstructured containers. *Small*. 2008; 4:1605–1609. [PubMed: 18702125]
29. Syms RRA, Yeatman EM. Self-assembly of three-dimensional microstructures using rotation by surface tension forces. *Electron Lett*. 1993; 29:662–664.
30. Gracias DH, et al. Fabrication of micrometer-scale, patterned polyhedra by self-assembly. *Adv Mater*. 2002; 14:235–238.
31. Leong TG, et al. Surface tension driven self-folding polyhedra. *Langmuir*. 2007; 23:8747–8751. [PubMed: 17608507]
32. Azam A, et al. Compactness determines the success of cube and octahedron self-assembly. *PloS One*. 2009; 4:e4451. [PubMed: 19212438]
33. Filipiak DJ, et al. Hierarchical self-assembly of complex polyhedral microcontainers. *J Micromech Microeng*. 2009; 19:1–6. [PubMed: 20161118]
34. Nix WD. Mechanical properties of thin films. *Metall. Trans. A, Phys. Metall. Mater. Sci*. 1989; 20:2217–2245.
35. Leong TG, et al. Self-loading lithographically structured microcontainers: 3D patterned, mobile microwells. *Lab Chip*. 2008; 8:1621–1624. [PubMed: 18813382]
36. Park JR, et al. Reconfigurable microfluidics with metallic containers. *J Microelectromech Syst*. 2008; 17:265–271.
37. Randall CL, et al. Size selective sampling using mobile, three-dimensional nanoporous membranes. *Anal Bioanal Chem*. 2009; 393:1217–1224. [PubMed: 19066861]
38. Randall CL, et al. Three-dimensional microwell arrays for cell culture. *Lab Chip*. 2011; 11:100–103. [PubMed: 20938497]
39. Ye H, et al. Remote radio-frequency controlled nanoliter chemistry and chemical delivery on substrates. *Angew Chem Int Ed Engl*. 2007; 46:4991–4994. [PubMed: 17508384]
40. Randall CL, et al. 3D lithographically fabricated nanoliter containers for drug delivery. *Adv Drug Deliv Rev*. 2007; 59:1547–1561. [PubMed: 17919768]
41. Gimi B, et al. Cell viability and noninvasive in vivo MRI tracking of 3D cell encapsulating self-assembled microcontainers. *Cell Transplant*. 2007; 16:403–408. [PubMed: 17658130]
42. Kalinin YV, et al. Three-dimensional chemical patterns for cellular self-organization. *Angew Chem Int Ed Engl*. 2011
43. Weaver VM, et al. Reversion of the malignant phenotype of human breast cells in three-dimensional culture and in vivo by integrin blocking antibodies. *J. Cell Biol*. 1997; 137:231–245. [PubMed: 9105051]
44. Wolf K, et al. Compensation mechanism in tumor cell migration: mesenchymal-amoeboid transition after blocking of pericellular proteolysis. *J. Cell Biol*. 2003; 160:267–277. [PubMed: 12527751]
45. Cukierman E, et al. Taking cell-matrix adhesions to the third dimension. *Science*. 2001; 294:1708–1712. [PubMed: 11721053]
46. Fischbach C, et al. Engineering tumors with 3D scaffolds. *Nat. Methods*. 2007; 4:855–860. [PubMed: 17767164]
47. Nelson CM, et al. Tissue geometry determines sites of mammary branching morphogenesis in organotypic cultures. *Science*. 2006; 314:298–300. [PubMed: 17038622]

48. Richardson TP, et al. Polymeric system for dual growth factor delivery. *Nat Biotechnol.* 2001; 19:1029–1034. [PubMed: 11689847]
49. Abbott A. Biology's new dimension. *Nature.* 2003; 424:870–872. [PubMed: 12931155]
50. Engler AJ, et al. Matrix elasticity directs stem cell lineage specification. *Cell.* 2006; 126:677–689. [PubMed: 16923388]
51. Feder-Mengus C, et al. New dimensions in tumor immunology: what does 3D culture reveal? *Trends Mol Med.* 2008; 14:3–40. [PubMed: 18055262]
52. Yuan J, et al. Electrospun three-dimensional hyaluronic acid nanofibrous scaffolds. *Biomaterials.* 2006; 27:3782–3792. [PubMed: 16556462]
53. Yang J, et al. Reconstruction of functional tissues with cell sheet engineering. *Biomaterials.* 2007; 34:5033–5043. [PubMed: 17761277]
54. Barry RA, et al. Direct-write assembly of 3D hydrogel scaffolds for guided cell growth. *Adv Mater.* 2009; 21:1–4.
55. Bassik N, et al. Patterning thin film mechanical properties to drive assembly of complex 3D structures. *Adv Mater.* 2008; 20:4760–4764.
56. Jamal M, et al. Directed growth of fibroblasts into three dimensional micropatterned geometries via self-assembling scaffolds. *Biomaterials.* 2010; 31:1683–1690. [PubMed: 20022106]
57. Nikishkov GP. Curvature estimation for multilayer hinged structures with initial strains. *J Appl Phys.* 2003; 94:5333–5336.
58. Bassik N, et al. Microassembly based on hands free origami with bidirectional curvature. *Appl Phys Lett.* 2009; 95:1–3.
59. Polychronidis A, et al. Twenty years of laparoscopic cholecystectomy: Philippe Mouret—March 17, 1987. *J Soc Laparoendoscopic Surg.* 2008; 12:109–111.
60. Hunter JG. Minimally invasive surgery: The next frontier. *World J Surg.* 1999; 23:422–424. [PubMed: 10030867]
61. Jaffray B. Minimally invasive surgery. *Arch Dis Child.* 2005; 90:537–542. [PubMed: 15851444]
62. Darzi A, Munz Y. The impact of minimally invasive surgical techniques. *Annu Rev Med.* 2004; 55:223–237. [PubMed: 14746519]
63. Muneer A, et al. Natural orifice transluminal endoscopic surgery: a new dimension in minimally invasive surgery. *Expert Rev Gastroenterol Hepatol.* 2008; 2:155–157. [PubMed: 19072349]
64. Sharma D, et al. Intraluminal robotics: a new dawn in minimally invasive surgery? *Br J Urol Int.* 2008; 102:265–266.
65. Nguyen N, et al. Single laparoscopic incision transabdominal (SLIT) Surgery—adjustable gastric banding: A novel minimally invasive surgical approach. *Obes Surg.* 2008; 18:1628–1631. [PubMed: 18830779]
66. Mack MJ. Minimally invasive and robotic surgery. *JAMA.* 2001; 285:568–572. [PubMed: 11176860]
67. Swanstrom L, et al. Developing essential tools to enable transgastric surgery. *Surg Endosc.* 2008; 22:600–604. [PubMed: 17973169]
68. Dhumane PW, et al. Minimally invasive single-site surgery for the digestive system: A technological review. *J Minim Access Surg.* 2011; 7:40–51. [PubMed: 21197242]
69. Leong TG, et al. Tetherless thermobiochemically actuated microgrippers. *Proc Natl Acad Sci USA.* 2009; 106:703–708. [PubMed: 19139411]
70. Bassik N, et al. Enzymatically triggered actuation of miniaturized tools. *J Am Chem Soc.* 2010; 132:16314–16317. [PubMed: 20849106]
71. Randhawa JS, et al. Pick-and-place using chemically actuated microgrippers. *J Am Chem Soc.* 2008; 130:17238–17239. [PubMed: 19053402]
72. Randhawa JS, et al. Reversible actuation of microstructures by surface chemical modification of thin film bilayers. *Adv Mater.* 2010; 22:407–410. [PubMed: 20217729]
73. Zakharchenko S, et al. Fully biodegradable self-rolled polymer tubes: A candidate for tissue engineering scaffolds. *Biomacromolecules.* 2011
74. Ionov L. Soft microorigami: self-folding polymer films. *Soft Matter.* 2011

75. Xia Y, Whitesides GM. Soft lithography. *Annu Rev Mater Sci.* 1998; 28:153–184.
76. Guan J, et al. Self-folding of hydrogel three dimensional microstructures. *J Phys Chem B.* 2005; 109:23134–23137. [PubMed: 16375273]
77. Gallego D, et al. Multilayer micromolding of degradable polymer tissue engineering scaffolds. *Mater Sci Eng: C.* 2008; 28:353–358.
78. Jager EWH, et al. Microfabricating Conjugated Polymer Actuators. *Science.* 2000; 24:1540–1545. [PubMed: 11090345]
79. Laflin KE, et al. Tetherless microgrippers with transponder tags. *J Microelectromech Syst.* 2011; 20:505–511.
80. Fernandes R, et al. Enabling cargo-carrying bacteria via surface attachment and triggered release. *Small.* 2011; 7:588–592. [PubMed: 21370460]

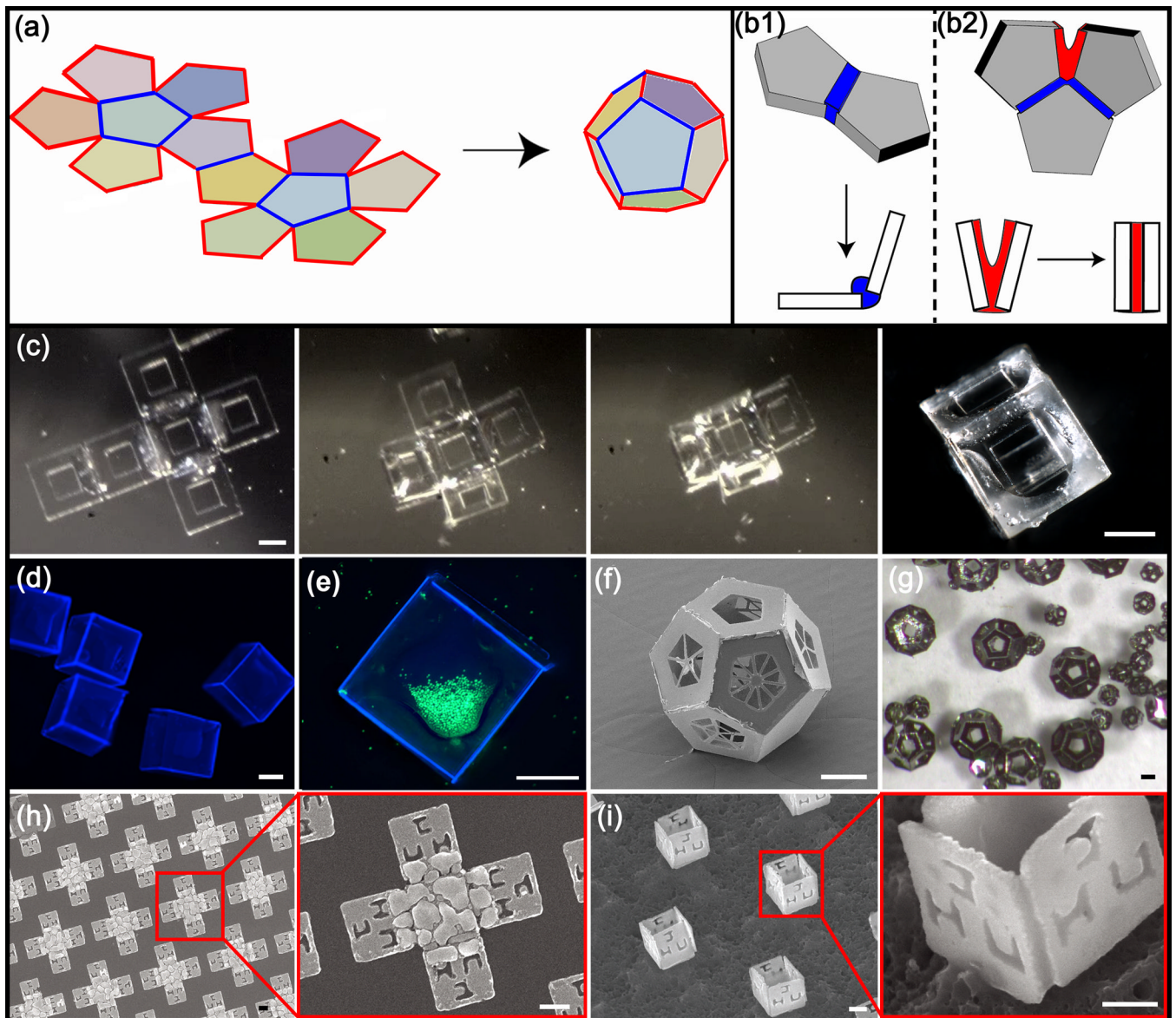


Figure 1. Schematic and versatility of the self-folding method for hollow polyhedral containers
 (a) Schematic showing 2D to 3D self-folding of a dodecahedron using surface tension based self-folding. The 2D template or net is patterned with hinges between panels (folding hinges) and also at the edges (locking hinges). (b) Schematics showing functionality of the two hinges, (b1) folding hinges provide a torque to rotate panels and (b2) locking hinges self-align and fuse panels at non-folding edges. Folding and locking are both driven by physical forces associated with the minimization of surface area of the molten hinge materials. *Adapted, with permission, Ref. [33] ©IOP Publishing Ltd.* (c) Video capture sequence (over 15 s) showing self-folding of a 1 mm sized, six-windowed polymeric container (with SU-8 panels and biodegradable polycaprolactone (PCL) hinges) on heating to 60°C. (d) Fluorescence image of a group of 1 mm sized SU8/PCL containers. (e) Fluorescence z-plane stack image of live, calcein stained fibroblast cells encapsulated within an optically transparent SU8/PCL container. *Reprinted, with permission, Ref. [26] ©Springer.* (f) SEM image of a self-folded dodecahedral shaped hollow metallic container featuring anisotropic surface patterning of slits. (g) Optical image of numerous 100 μm, 200

μm and $500\ \mu\text{m}$ (panel edge length) dodecahedra, highlighting that many containers can be fabricated en masse. *Reprinted, with permission, Ref. [33] ©IOP Publishing Ltd.* (h–i) SEM images of electron-beam patterned 2D templates and self-folded $100\ \text{nm}$ scale cubic particles. It should be noted that the self-folding process is parallel even at the nanoscale and the particles have the letters JHU patterned with line widths as small as $15\ \text{nm}$. These particles have been created with both metallic (nickel) and ceramic (alumina) panel composition. *Reprinted, with permission, Ref. [25] ©American Chemical Society 2009.* The scale bars: (a–e) $500\ \mu\text{m}$ and (f–d) $250\ \text{nm}$ long.

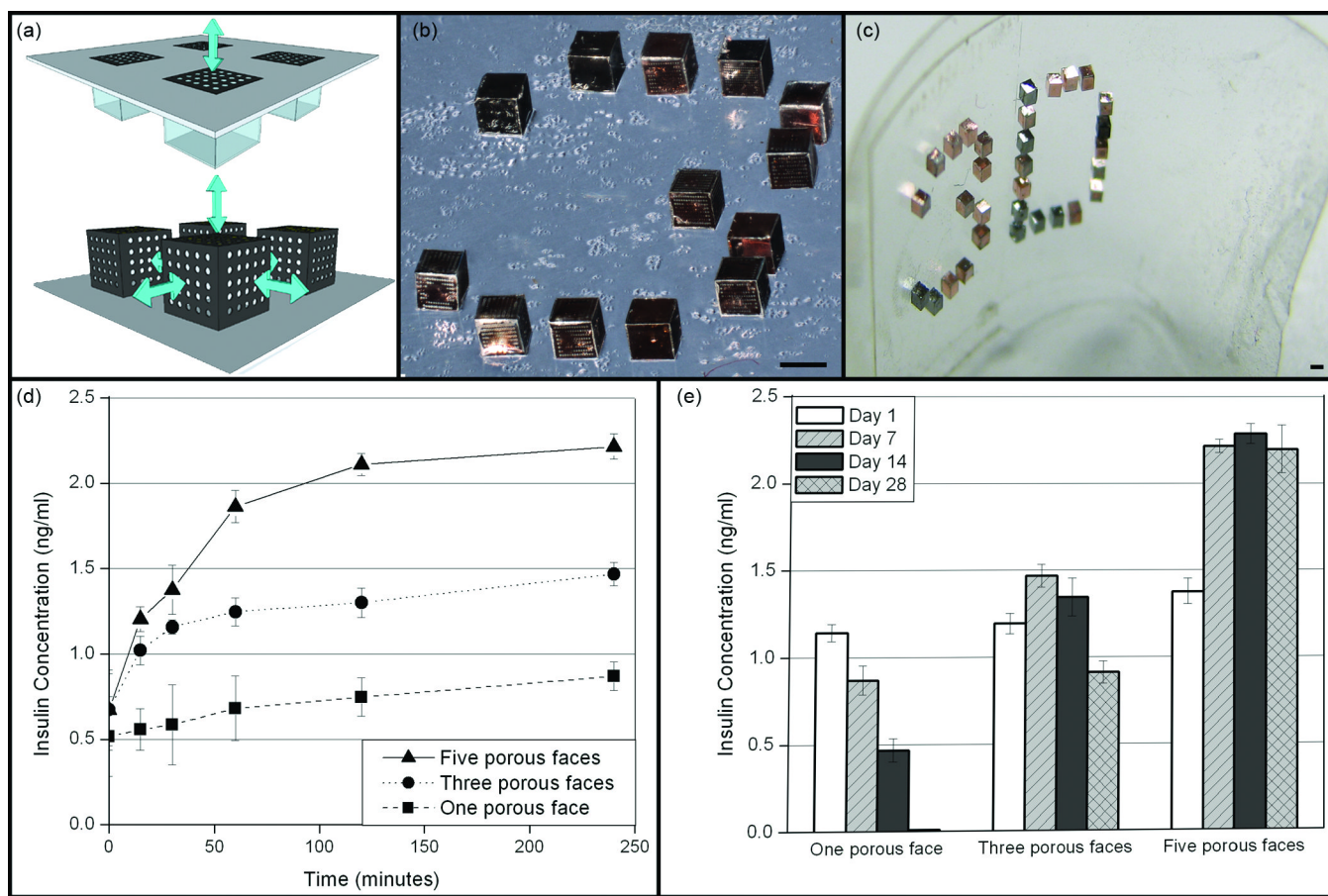


Figure 2. Versatile design of 3D microwell arrays composed of self-folding devices for enhanced diffusion in biomedical applications

(a). Conceptual schematic of a conventional 2D microwell array (top) and our 3D microwell array (bottom). The important difference is that although both are 3D recesses, microfabricated 2D microwell arrays feature well defined porosity only along one surface. (b–c) Optical images of ordered 3D microwell arrays composed of Au-coated containers on both (b) flat polyurethane coated silicon and (c) curved polymeric surfaces. The number “3” and letter “D” are spelt out to highlight versatility in the spacing and positioning offered by this technique. All scale bars are 500 μm long. (d) Insulin response profiles to a glucose stimulation from one, three and five porous-faced microwell arrays after seven days. Data are plotted as the average \pm the standard deviation (sample size $n = 5$). (e) A graph showing the four hour (steady-state) insulin concentration measured in response to a glucose stimulation for β -TC-6 cells encapsulated within 2D (one porous-faced), three porous-faced and 3D (five porous-faced) microwell arrays. The average and the standard deviation obtained on days 1 (number of samples, $n = 5$), 7 ($n = 5$), 14 ($n = 3$) and 28 ($n = 3$) are plotted. The 3D microwell arrays produced significantly greater stimulated insulin at longer times. Reprinted, with permission, Ref. [38] ©The Royal Society of Chemistry.

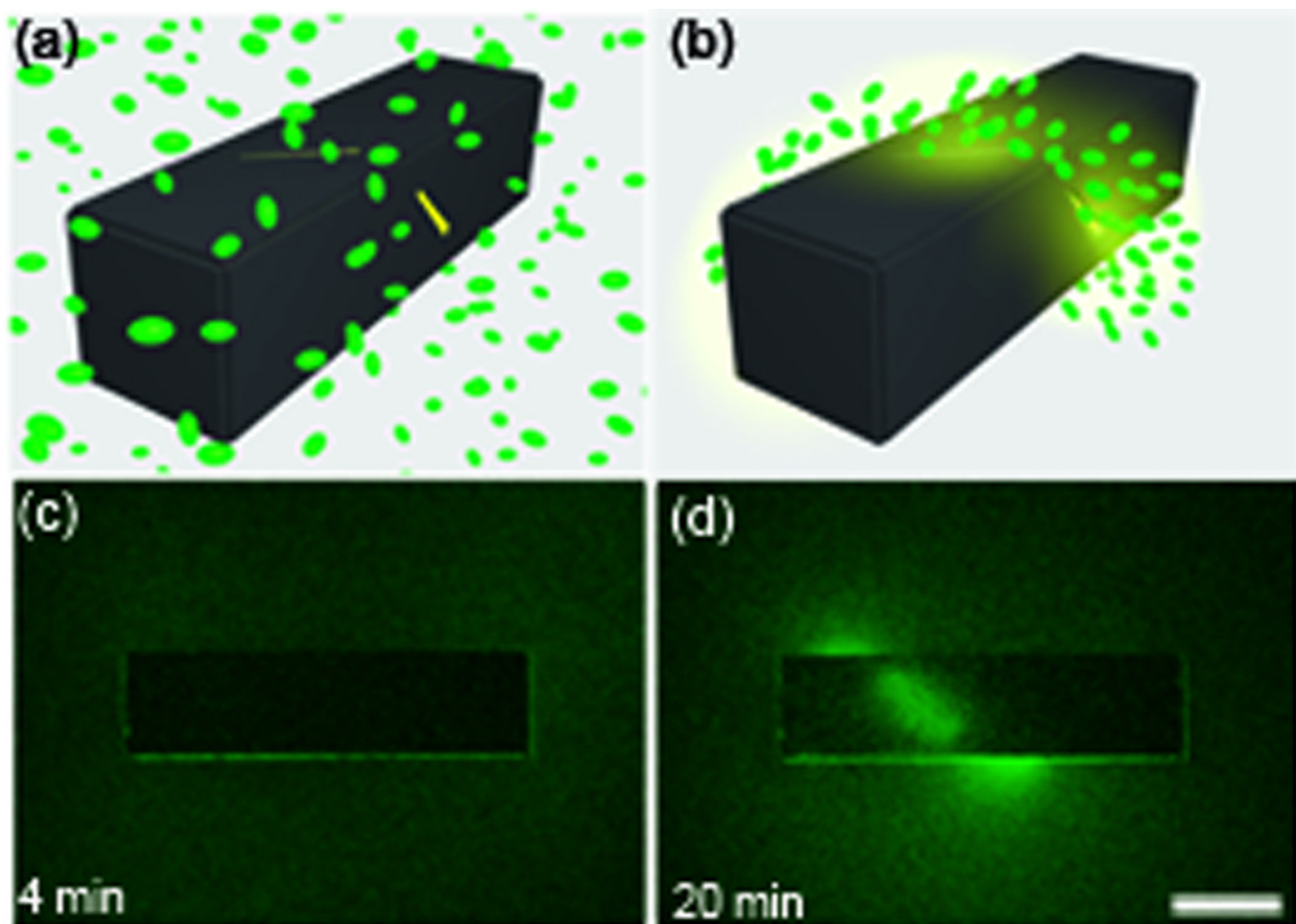


Figure 3. Using containers with precisely patterned wall porosity to direct the chemotactic self-organization of *E. coli* in the shape of a helix
 (a–b). A conceptual schematic of the desired chemotactic self organization in a spiral. At the start of the experiment, a) the chemoattractant is confined to the Au-coated container and green fluorescent protein (GFP) expressing *E. coli* cells are distributed uniformly throughout the medium. b) *E. coli* cells self-organize in a helical pattern based on the underlying chemical pattern once the chemoattractant (L-serine, yellow) is allowed to diffuse out of the container. (c–d) Experimental realization of the concept. Time-lapse images of green fluorescent *E. coli* as they self-organized in a helical pattern around a container. The scale bar is 500 μm long. Adapted and reprinted with permission, Ref. [42] ©Wiley-VCH Verlag GmbH & Co. KgaA.

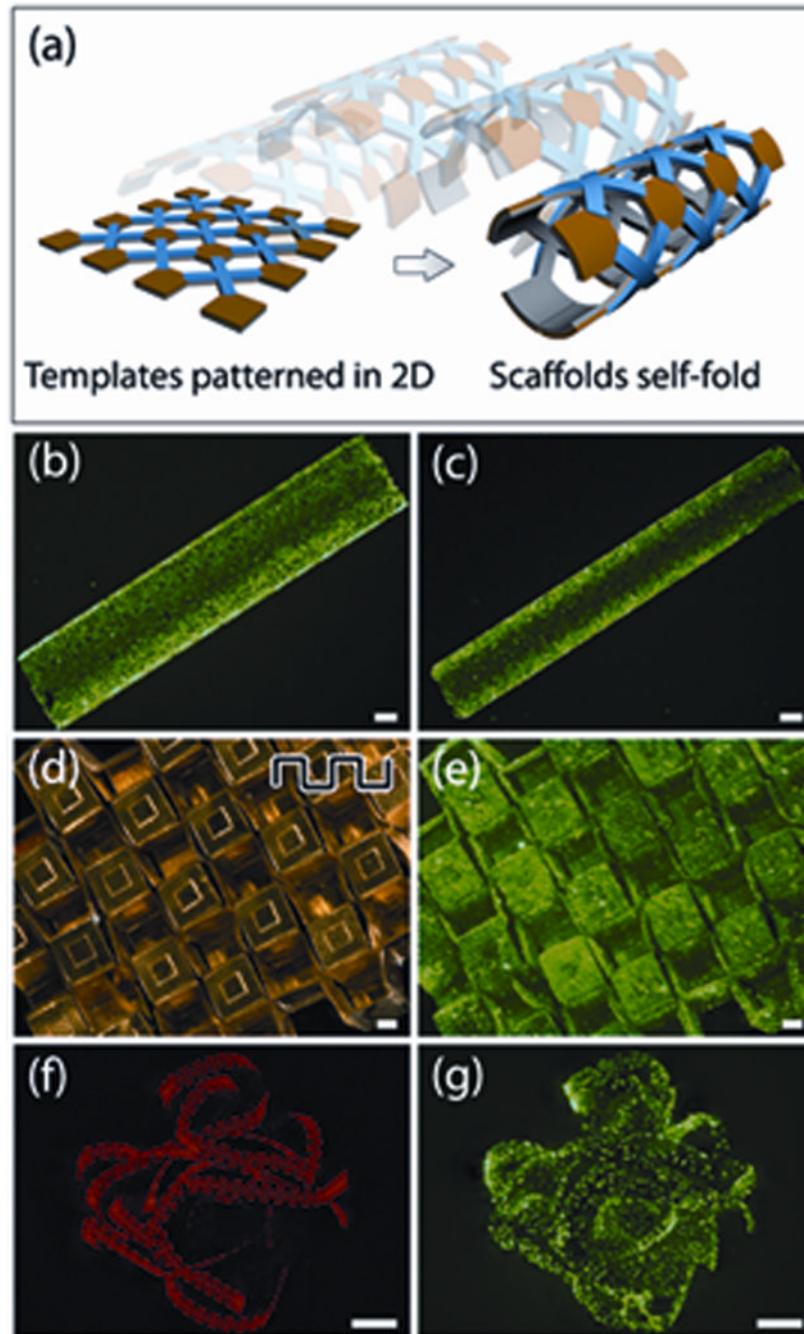


Figure 4. Self-folding scaffolds in anatomically relevant geometries

(a) Schematic of self-folding of planar, micropatterned templates from 2D to 3D geometries on release from the substrate. (b–c) Fluorescent image of a calcein stained cell culture grown on cylindrical scaffolds of two different diameters. The cylinders consist of a 15×15 array of $160 \mu\text{m}$ square panels spaced $80 \mu\text{m}$ apart. (d–e) Optical images of a bi-directionally folded scaffold and fluorescently labeled fibroblasts cultured on it. Schematic overlay illustrates the undulatory cross-section of the scaffold. (f–g) Optical images of a self-folding spiral-like ribbon and calcein stained fibroblasts cultured on it. The scale bars are $160 \mu\text{m}$ long. *Adapted and reprinted with permission, Ref. [56] ©Elsevier, 2010.*

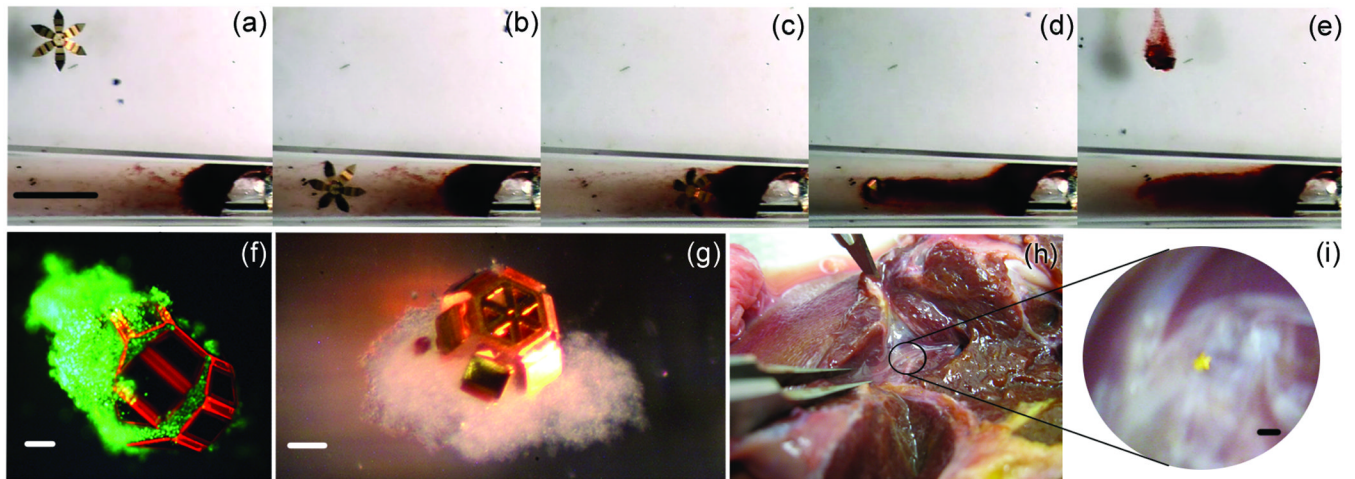


Figure 5. Self-folding miniaturized tools for surgery

(a–e) Optical microscopy sequence showing capture and retrieval of neutral red-stained cells from a cell culture mass at the end of a tube; the scale bar is 1 mm long. (f) Fluorescent micrograph of viable (green) L929 cells captured by using a biochemical trigger to actuate the gripper; the scale bar is 100 μm long. (g) Optical image of a microgripper with a tissue sample retrieved from a bovine bladder; the scale bar is 100 μm long. *Adapted and reprinted with permission, Ref. [69].* (h, i) Body temperature activated microgrippers in intrahepatic porcine bile ducts, ex-vivo, The scale bar is 1 mm long.

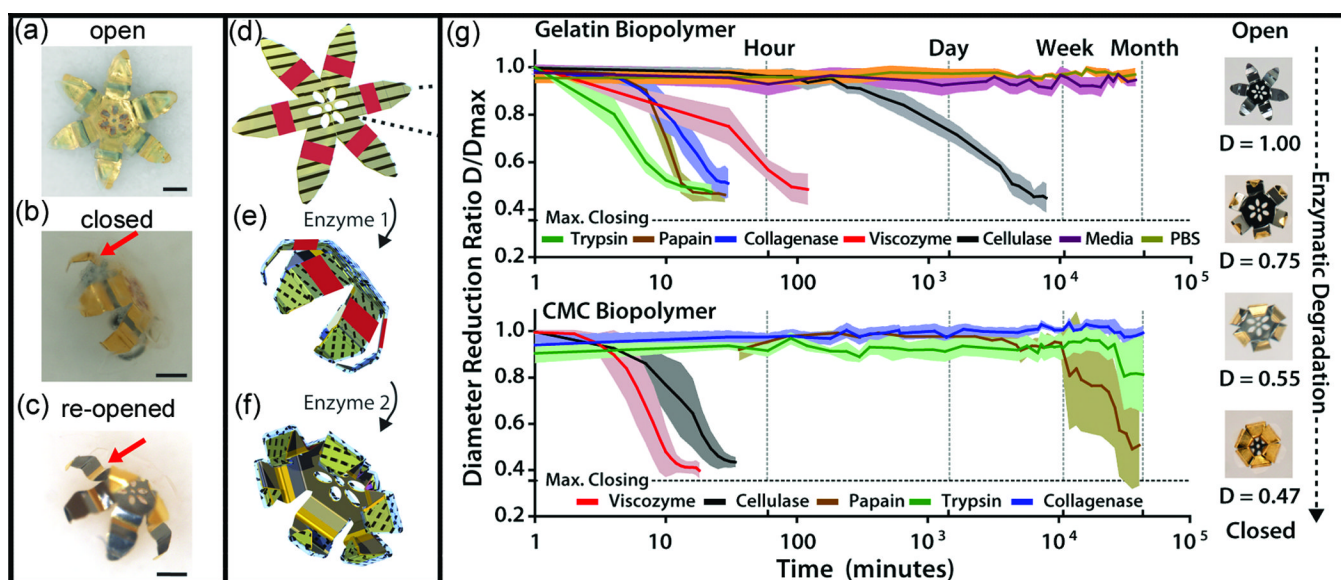


Figure 6. Surgical tools that close and open when exposed to enzymes

(a–c) Optical images of a microgripper patterned with gelatin (a polypeptide) and carboxymethylcellulose (CMC, a polysaccharide) triggers in three different states: open (as fabricated), closed (on exposure to cellulase), and re-opened (on exposure to proteases such as collagenase). The red arrow indicates the set of hinges that cause re-opening. The scale bars are 200 μm long. (d–f) Schematic conceptual representations of the grippers in the three corresponding states. (d) The gripper is kept flat by the biopolymer layers. (e) When one biopolymer is selectively degraded by a specific enzyme class (enzyme 1) the gripper closes. (f) Subsequently, a second set of hinges, which are insensitive to enzyme 1 are actuated by another enzyme class (enzyme 2) and the gripper re-opens (g) Plots of the kinetics of gripper closing on exposure to different enzymes indicating cross-selectivity of over two orders of magnitude. *Adapted and reprinted with permission, Ref. [70] ©American Chemical Society, 2009.*